

FORMATION OF STATIONARY MAGNETOHYDRODYNAMIC OUTFLOWS FROM A DISK BY TIME-DEPENDENT SIMULATIONS

M. M. ROMANOVA

Space Research Institute, Russian Academy of Sciences, Moscow, Russia, and Department of Astronomy, Cornell University,
 Ithaca, NY 14853-6801; romanova@astrosun.tn.cornell.edu

G. V. USTYUGOVA, A. V. KOLDOBA, AND V. M. CHECHETKIN

Institute of Applied Mathematics, Russian Academy of Sciences, Moscow, Russia

AND

R. V. E. LOVELACE

Department of Astronomy, Cornell University, Ithaca, NY 14853-6801; rv11@cornell.edu

Received 1996 June 20; accepted 1997 February 20

ABSTRACT

We report the discovery of a family of stationary magnetohydrodynamic (MHD) outflows from a disk found by time-dependent, axisymmetric MHD simulations. The initial poloidal magnetic field threading the disk was taken to be a tapered monopole field, with the field strength on the disk decreasing outwardly to small values. At the disk surface, matter was given a small initial push with a speed less than the slow magnetosonic speed. In the simulations, the outflowing matter is observed to be accelerated by magnetic and centrifugal forces up to velocities in excess of the fast magnetosonic speed and in excess of the escape speed.

Subject headings: ISM: jets and outflows — MHD

1. INTRODUCTION

Magnetohydrodynamic (MHD) outflows from accretion disks are a likely explanation of the origin of astrophysical jets. Analytic solutions for stationary MHD outflows predict that the field lines at the disk surface diverge away from the symmetry axis and that the driving force acting to overcome the gravitational pull of the central object is the component of centrifugal force along the magnetic field (Blandford & Payne 1982) or the magnetic pressure gradient force (Lovelace, Berk, & Contopoulos 1991; hereafter LBC). However, the analytical models involve major assumptions (self-similar scaling of the magnetic field; Blandford & Payne 1982) and approximations (averaging over the jet cross section; LBC) that limit their applicability to real systems. Numerical simulations provide a method for obtaining further understanding of MHD outflows and jets.

Axisymmetric numerical simulations of matter outflows from a cold accretion disk performed by Uchida & Shibata (1985) showed the possibility of nonstationary magnetically driven outflows from an accretion disk. Analogous simulations were performed by Stone & Norman (1994), who concentrated on processes inside the disk, and by Bell & Lucek (1995). Matsumoto et al. (1997) studied nonstationary outflows using three-dimensional MHD simulations. In these simulations, the back-reaction of the outflows on the disk led to the rapid collapse of the disk, which prevented investigation of the behavior of the outflows over an extended period of time.

Another approach was taken by Ustyugova et al. (1995), Koldoba et al. (1995), and Meier, Payne, & Lind (1997), who performed axisymmetric numerical simulations of outflows from accretion disks considered as a boundary condition. In this approach, an outflow is assumed to originate from an outer “coronal” layer of the disk which has a higher temperature and lower density than the disk mid-plane. This layer is referred to as the disk surface. In this

approach it is supposed that the outflow occurs on the upper layer of the disk without a major change in the structure of the disk. This permits a study of the outflows during much longer times. However, in the reported studies only nonstationary, transitory outflows were observed.

Here we present results of time-dependent, axisymmetric, numerical MHD simulations in which stationary outflows from the disk considered as a boundary condition were obtained, starting from different nonequilibrium states and from different physical parameters on the disk. This work was briefly described by Lovelace & Romanova (1996). Compared to our earlier work (Ustyugova et al. 1995) in which only nonstationary outflows were observed, here the magnetic field at the disk is much stronger.

2. DESCRIPTION OF THE PROBLEM

Axisymmetric MHD outflows from the disk surface are treated using the equations for ideal, isothermal MHD flows,

$$\frac{\partial \rho}{\partial t} + \nabla \cdot (\rho \mathbf{v}) = 0, \quad (1)$$

$$\frac{\partial \mathbf{v}}{\partial t} + (\mathbf{v} \cdot \nabla) \mathbf{v} + \frac{1}{\rho} \nabla p - \mathbf{g} - \frac{1}{4\pi\rho} (\nabla \times \mathbf{B}) \times \mathbf{B} = 0, \quad (2)$$

$$\frac{\partial \mathbf{B}}{\partial t} - \nabla \times (\mathbf{v} \times \mathbf{B}) = 0. \quad (3)$$

Here ρ is the mass density, $\mathbf{v} = (v_r, v_\phi, v_z)$ is the flow velocity, $\mathbf{B} = (B_r, B_\phi, B_z)$ is magnetic field, $p = \rho c_s^2$ is the pressure, c_s is isothermal sound speed, and $\mathbf{g} = -\nabla\Phi_g$ is the gravitational acceleration. A gravitating body (a star or black hole) of mass M is located at the center ($r = 0, z = 0$) of the disk. We neglect the self-gravity of the disk. We smoothed the gravitational potential by taking $\Phi_g = -GM/(r^2 + r_i^2)^{1/2}$, where r_i is the characteristic radius which we refer to as the inner radius of the disk. This radius has a natural interpre-

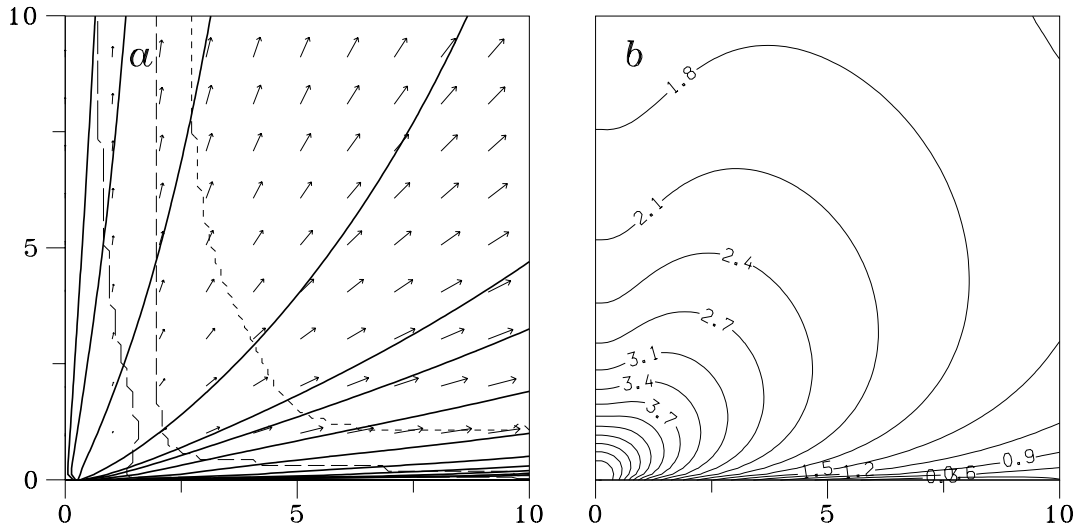


FIG. 1.—(a) Poloidal magnetic field (solid lines) and poloidal velocities (vectors) for the run with initial parameters $(v_A/v_K)_i = 0.9$ and $(c_s/v_K)_i = 0.5$, and $\eta = 2$ at $t = 100t$, when a stationary outflow was established. The long dashed line is the slow magnetosonic surface, the dashed line is the Alfvén surface, and the short dashed line is the fast magnetosonic surface. The poloidal velocity vectors are not exactly aligned with the poloidal magnetic field, but the angle between the vectors is $< 5^\circ$. For ideal axisymmetric MHD flows this angle is zero in a stationary state (Lovelace et al. 1986). (b) Logarithm of the density contours for the flow at the same time.

tation as the inner radius of the disk. The disk rotates with Keplerian velocity $v_K^2 = GMr^2/(r^2 + r_i^2)^{3/2}$.

We push matter out from the disk surface with a small velocity equal to a fraction $\alpha < 1$ of the slow magnetosonic velocity, as discussed by Ustyugova et al. (1995). Note that the density of matter outflowing from the disk surface is *not* fixed but rather adjusts to satisfy the MHD equations above the disk.

Because the plasma outflows from the disk with sub-slow magnetosonic velocity, only three boundary conditions are needed at the $z = 0$ surface. One boundary condition is this outflow velocity. The other two boundary conditions result from the disk's being perfectly conducting: the tangential electric field in the reference frame comoving with the disk vanishes, $[(v - v_K) \times B]_{r,\phi} = 0$, where $v_K = v_K \hat{\phi}$.

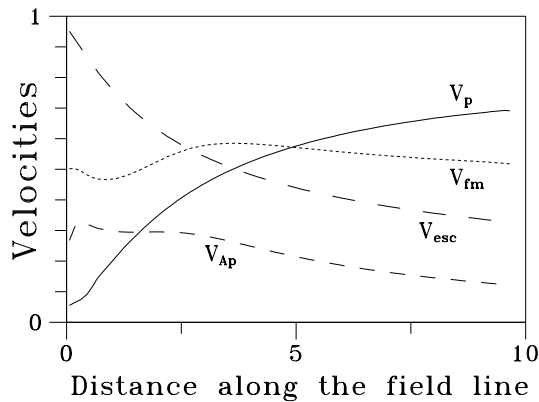


FIG. 2.—Velocities along a magnetic field line, the sixth line away from the axis in Fig. 1a. Here V_p is poloidal velocity of the flow; V_A is the Alfvén velocity; V_{fm} is the fast magnetosonic velocity; V_{esc} is the local velocity of escape.

On top of the considered region at $z = Z_{max}$ and on the right side of the region $r = R_{max}$ we take free boundary conditions $\partial F_j/\partial z = 0$ and $\partial F_j/\partial r = 0$ for all variables F_j excluding the toroidal magnetic field. In contrast with the “free” outer boundary condition on B_ϕ used in our previous work (Ustyugova et al. 1995), we took $(B_p \cdot \nabla)rB_\phi = 0$. This condition means that the poloidal current density J_p is parallel to the poloidal field B_p at the outer boundaries. Thus, on these boundaries the magnetic force in the ϕ -direction vanishes. The “free” boundary condition on B_ϕ gives on the top boundary the condition $J_r \propto \partial B_\phi/\partial z = 0$, which means that the current flows across the boundary in the z -direction. Interaction of this current with B_r leads to an unphysical winding of the field near the boundary. This phenomenon is connected with rectangular shape of the simulation region and vanishes in the case of the spherical region. Note also that the outer boundary conditions are unimportant once the flow becomes super-fast magneto-

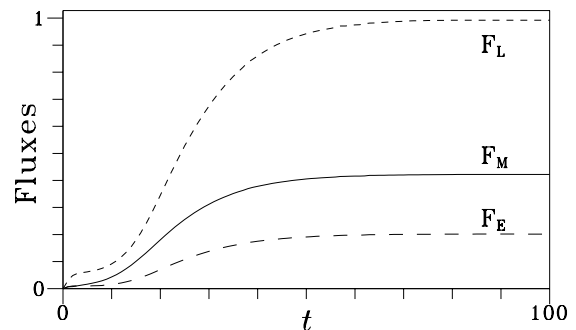


FIG. 3.—Fluxes through the surface $z = Z_{max}/2$ vs. time t . Here F_M is the mass flux, F_L is the total angular momentum flux (about the z -axis), and F_E is the total energy flux. The scales are arbitrary. Time is measured in units of t_r , which is the period of rotation at the inner edge of the disk (r_i).

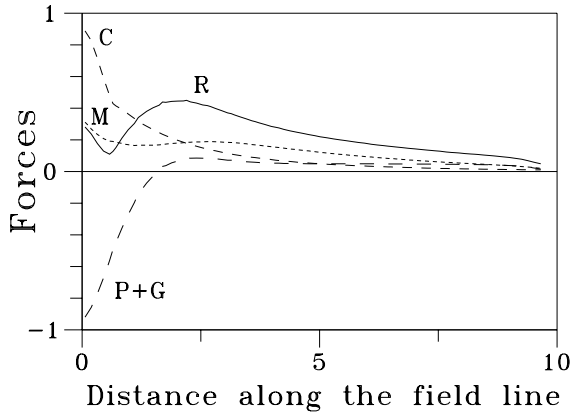


FIG. 4.—Forces acting along the same magnetic field line as in Fig. 2, at $t = 100t_i$. The gravitational force is denoted G ; the centrifugal force is C ; the sum of thermal pressure gradient force and gravity force is $P + G$; the magnetic force is M ; and the resultant force $R = G + C + P + M$.

sonic. Also we include damping of any waves propagating down from the top boundary.

The objective of this work was to find stationary super-fast magnetosonic outflows driven by magnetic and/or centrifugal forces. Since we do not know the parameters of the system in the stationary state in advance, we started from nonequilibrium initial conditions: For the gas, we assumed an equilibrium in the gravitational field, $(1/\rho)\nabla p = g$. For the magnetic field, we assumed a “tapered” monopole field,

$$\mathbf{B}_p = \mathbf{B}_m / [1 + \eta \tan^2(\theta)], \quad (4)$$

where \mathbf{B}_p is the poloidal magnetic field, \mathbf{B}_m is the field of the monopole, θ is the angle between the magnetic field lines

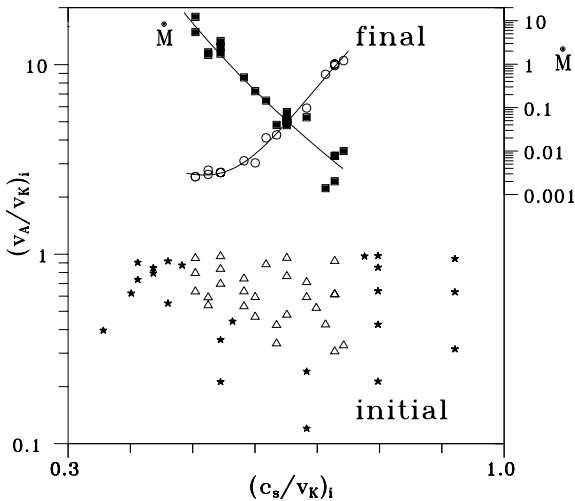


FIG. 5.—Initial and final parameters of different simulation runs for $\eta = 9$. Triangles are initial parameters of runs which led to stationarity, and stars are for the cases which did not lead to stationarity. Circles are final parameters of stationary runs, and the solid curve is the smooth fit through these values. The filled squares represent the mass efflux from the disk for the stationary solutions. The scale for \dot{M} is arbitrary. The stationary solutions are located between $0.5 \lesssim (c_s/v_K)_i \lesssim 0.73$. At the high c_s limit, \dot{M} is very small, and the angle between the magnetic field lines near the disk and the disk surface is about 30° . On the other hand, at the low c_s limit \dot{M} is large and the angle between the field lines and the disk is small, $\sim 7^\circ$.

and the z -axis, and η is a parameter which determines the degree of tapering. Tapering was introduced to decrease the collimating effect of the toroidal magnetic field at large r on the disk which develops as t increases. Initially, the toroidal magnetic field is zero everywhere. We have studied cases with $\eta = 0-9$. The monopole was located beneath the disk at $z = -2.5r_i$.

For the numerical solution of equations (1)–(3), we used a TVD numerical scheme of Godunov’s type which was described by Koldoba et al. (1995). This scheme is analogous to that proposed by Brio & Wu (1988) for the adiabatic case. The MHD code passed a number of tests, including tests of slow, fast, and Alfvén wave propagation and tests involving contact discontinuities and shock waves. The tests demonstrated good correspondence between numerical and exact solutions.

We treated the region $r \leq R_{\max} = 10r_i$, $z \leq Z_{\max} = 10r_i$, and number of grid points $N_r = 80$ and $N_z = 80$. A typical successful run giving a stationary solution took about 100 hr on a 166 MHz Pentium computer.

3. RESULTS

We calculated more than 50 different cases with different initial parameters $(v_A/v_K)_i$ and $(c_s/v_K)_i$, where $(v_A)_i \equiv (B^2/4\pi\rho)_i^{1/2}$ is Alfvén velocity at radius $r = r_i$ at the disk surface [not the disk midplane where $v_A(0) \ll v_K$] and discovered that in some cases the flow becomes stationary and in other cases it does not.

Figures 1, 2, and 4 show results for one successful run at a late time when the jet is stationary for $(v_A/v_K)_i = 0.9$ and $(c_s/v_K)_i = 0.5$. Figure 1a shows the poloidal velocity vectors and poloidal magnetic field. Figure 1b shows density contours. Figure 2 shows the variation of different velocities along one inclined magnetic field line. One can see from Figures 1a and 2 that the flow is accelerated and passes through the slow magnetosonic, Alfvénic, and fast magnetosonic surfaces. Also, note that the velocity becomes higher than the local escape velocity. One can see that matter is accelerated mainly in the region near the gravitational center where the magnetic field is strong. The flow is essentially uncollimated in the simulation region.

Figure 3 shows variation with time fluxes of mass, angular momentum, and energy integrated across the surface $z = Z_{\max}/2$. The fluxes initially grow, but later, after a period $\sim 50t_i$, they become stationary. Simulations for longer times (up to $150t_i$) confirmed that the fluxes are stationary. The stationary condition of the fluxes at the outer boundaries reflects also the fact that matter outflow from the disk becomes stationary, that is, the density distribution of matter along the disk becomes fixed. Here $t_i = 2\pi r_i/v_{K_i}$ is the period of the disk rotation at $r = r_i$.

Analysis of the forces shows that the matter is accelerated by a combination of magnetic and centrifugal forces in the region of inclined magnetic field lines (Fig. 4). However, near the axis, the thermal pressure gradient force is also important for driving matter out from gravitational center. This determined the fact that there are no stationary solutions for $(c_s/v_K)_i < 0.5$ (Fig. 5).

The area of initial and final parameters of the flow is shown in Figure 5 in the diagram $(v_A/v_K)_i$ versus $(c_s/v_K)_i$, where v_{A_i} is Alfvén velocity at the radius r_i at the surface of the disk (not the disk midplane). Each point corresponds to separate run. One can see that for a wide range of initial parameters, the final parameters corresponding to station-

ary outflows are located along a line which is above the initial $(v_A/v_K)_i$ values. We note that the Alfvén velocity (v_A), may be comparable or larger than Keplerian velocity because of the low density of matter at the surface of the disk. Evolution goes along vertical lines upward in the direction of higher Alfvén velocities. Note that simulations of different cases with the same sound speed and different Alfvén velocities lead to the final state with the same Alfvén velocity. All parameters of stationary solutions lie above the line $(v_A/v_K)_i \approx 3$. We observe that the flow becomes stationary if it passes through the fast magnetosonic surface in the early stages of the simulations.

4. DISCUSSION

In this paper, stationary MHD outflows from a disk have been found by time-dependent axisymmetric simulations. The initial magnetic field was taken to be a tapered monopole field. A family of such solutions has been studied for different magnetic field strengths and different temperatures. The main driving forces acting to overcome gravity and accelerate the outflowing matter are magnetic pressure gradient force and centrifugal force. The flows pass through all critical surfaces, including the fast magnetosonic surface, and reach velocities in excess of the escape speed. The direction of the poloidal flow and the poloidal B -field become aligned gradually as t increases. For ideal, axisymmetric, stationary MHD flows the two vectors are exactly aligned (see, for example, Lovelace et al. 1986).

We also performed simulations for the case of untapered initial monopole fields ($\eta = 0$) and obtained stationary outflows, but only for much stronger magnetic fields, $(v_A/v_K)_i \gg 1$. In this case matter was accelerated in the computational region to super-Alfvénic velocities and to escape velocities, but not to super-fast magnetosonic velocities.

In this paper we focused on the problem of the acceleration of matter by magnetic and/or centrifugal forces and

the problem of numerical investigation of the possibility of escape from the gravitational center mainly as a result of the action of these forces. In the region considered beyond the fast magnetosonic surface the kinetic energy density of matter is much higher than the energy density of the magnetic field, so that we cannot expect a strong collimation in this region. However, at far distances, the flow may be collimated by the pressure of an external medium (see LBC).

There is a principal difference of these results and those of our earlier work (Ustyugova et al. 1995; Koldoba et al. 1995), where we considered cases in which the magnetic energy density was much less than matter energy density, $\beta = c_s^2/v_A^2 \gg 1$. In this limit, the initial rotation of the disk generates a strong toroidal field in the corona which strongly collimates the outflowing matter, “turns off” both the magnetic and centrifugal driving forces, and prevents the occurrence of stationary solutions. Here we considered the opposite limit where $\beta < 1$ and the collimation of the flow is greatly reduced. Also, tapering of the initial magnetic field acts to decrease the collimating influence of the toroidal magnetic field.

One objective of our future work is to study the collimation of the stationary outflows using larger computational regions.

In this issue, Ouyed & Pudritz (1997) report stationary outflows from a disk treated as a boundary condition following Ustyugova et al. (1995).

We thank several referees for helpful comments on earlier versions of this paper. We also thank the Cornell Theory Center for supercomputer time. The authors were supported in part by NSF grant AST 93-20068. The Russian authors were also supported in part by the Russian Fundamental Research Foundation grant No. 1996-02-17113. The work of R. V. E. L. was supported in part by NASA grant NAGW 2293.

REFERENCES

- Bell, A. R., & Lucek, S. G. 1995, MNRAS, 277, 1327
 Blandford, R. D., & Payne, D. G. 1982, MNRAS, 199, 883
 Brio, M., & Wu, C. C. 1988, J. Comput. Phys., 75, 400
 Koldoba, A. V., Ustyugova, G. V., Romanova, M. M., Chechetkin, V. M., & Lovelace, R. V. E. 1995, Ap&SS, 232, 241
 Lovelace, R. V. E., Berk, H. L., & Contopoulos, J. 1991, ApJ, 379, 696
 Lovelace, R. V. E., Mehanian, C., Mobarry, C. M., & Sulkanen, M. E. 1986, ApJS, 62, 1
 Lovelace, R. V. E., & Romanova, M. M. 1996, in ASP Conf. Proc. 100, Energy Transport in Radio Galaxies and Quasars, ed. P. E. Hardee, A. H. Bridle, & J. A. Zensus (San Francisco: ASP), 25
 Matsumoto, R., et al. 1996, in IAU Colloq. 163, Accretion Phenomena and Related Outflows, ed. D. Wickramasinghe, L. Ferrario, & G. Bicknell (San Francisco: ASP), in press
 Meier, D. L., Payne, D. G., & Lind, K. R. 1996, in IAU Symp. 175, Extragalactic Radio Sources, ed. R. Ekers, C. Fanti, & L. Padrielli (Dordrecht: Reidel), in press
 Ouyed, R., & Pudritz, R. 1997, ApJ, 482, 712
 Stone, J. M., & Norman, M. L. 1994, ApJ, 433, 746
 Uchida, Y., & Shibata, K. 1985, PASJ, 37, 515
 Ustyugova, G. V., Koldoba, A. V., Romanova, M. M., Chechetkin, V. M., & Lovelace, R. V. E. 1995, ApJ, 439, L39